J. Fluid Mech. (2016), *vol.* 806, *pp.* 627–648.
doi:10.1017/jfm.2016.614

Kazantsev model in non-helical 2.5-dimensional flows

K. Seshasayanan[1,†] and A. Alexakis[1]

[1]Laboratoire de Physique Statistique, École Normale Supérieure, PSL Research University; Université Paris Diderot Sorbonne Paris-Cité; Sorbonne Universités UPMC Univ Paris 06; CNRS; 24 rue Lhomond, 75005 Paris, France

(Received 5 July 2016; revised 12 September 2016; accepted 17 September 2016; first published online 13 October 2016)

We study the dynamo instability for a Kazantsev–Kraichnan flow with three velocity components that depend only on two dimensions $\boldsymbol{u} = (u(x, y, t), v(x, y, t), w(x, y, t))$ often referred to as 2.5-dimensional (2.5-D) flow. Within the Kazantsev–Kraichnan framework we derive the governing equations for the second-order magnetic field correlation function and examine the growth rate of the dynamo instability as a function of the control parameters of the system. In particular we investigate the dynamo behaviour for large magnetic Reynolds numbers Rm and flows close to being two-dimensional and show that these two limiting procedures do not commute. The energy spectra of the unstable modes are derived analytically and lead to power-law behaviour that differs from the three-dimensional and two-dimensional cases. The results of our analytical calculation are compared with the results of numerical simulations of dynamos driven by prescribed fluctuating flows as well as freely evolving turbulent flows, showing good agreement.

Key words: dynamo theory, MHD and electrohydrodynamics, MHD turbulence

1. Introduction

Dynamo instability refers to the amplification of magnetic fields by the flow of a conducting fluid. It is responsible for the existence of magnetic fields in most astrophysical bodies. In most situations the driving flow is turbulent and this prevents an analytical treatment of the problem. Thus most studies are restricted to large-scale numerical simulations or simplified models. A simple flow that can be treated analytically is the Kazantsev–Kraichnan flow. This model considers the kinematic dynamo instability driven by a random velocity field that is homogeneous, delta correlated in time and Gaussian distributed. It was first examined by Kazantsev (1968) for the dynamo instability and was independently studied by Kraichnan (1968) for the problem of passive scalar advection. Physically, the delta-correlated time behaviour models the fast varying turbulent scales of the velocity field. Under these assumption the problem can be simplified to a one-dimensional eigenvalue problem, the eigenvalue of which gives the growth rate of the magnetic energy.

The Kazantsev–Kraichnan flow has been widely studied for three-dimensional isotropic flows. Since the velocity field is Gaussian distributed its statistics is entirely

†Email address for correspondence: skannabiran@lps.ens.fr

given by the second-order correlation function. The correlation function $g^{ij}(\boldsymbol{r})$ of the velocity field is defined as $\langle u^i(\boldsymbol{x}+\boldsymbol{r},t)u^j(\boldsymbol{x},t')\rangle = g^{ij}(\boldsymbol{r})\delta(t-t')$ where due to homogeneity the function g^{ij} is independent of $\boldsymbol{x}$. The first study by Kazantsev considered a flow for which the correlation function scales like $|g^{ii}(r)| \sim r^{\zeta}$ with ζ being the Hölder exponent. He found the existence of dynamo instability in the range $1<\zeta\leqslant 2$ for large Rm. Flows with Hölder exponents $\zeta<2$ correspond to rough flows and model the turbulent scales while flows with $\zeta=2$ correspond to smooth velocity fields that model the viscous scales where the nonlinearities are in balance with the viscous dissipation. Since then various authors (Ruzmaikin & Sokolov 1981; Novikov, Ruzmaikin & Sokoloff 1983; Falkovich, Gawdzki & Vergassola 2001; Schekochihin, Boldyrev & Kulsrud 2002; Vincenzi 2002) have considered velocity fields with both a turbulent inertial range and a viscous-scale cutoff at various limits of the system. For smooth flows $\zeta=2$, Chertkov *et al.* (1999) calculated the higher-order moments and multipoint correlation functions by means of a Lagrangian approach. Geometric properties of the advected field were examined by Boldyrev & Schekochihin (2000) and the effect of nonlinearities were examined in Boldyrev (2001). More recently the predictions of the model as well as the nonlinear behaviour have been examined by means of three-dimensional numerical simulations (Schekochihin *et al.* 2004; Iskakov *et al.* 2007; Mason *et al.* 2011).

There is a major difference between a two-dimensional (2-D) flow and a three-dimensional (3-D) flow concerning the dynamo instability. 2-D flows do not lead to a dynamo instability for any value of the magnetic Reynolds number as shown by Zeldovich (1957). This is also true in the 2-D Kazantsev model that has been examined in detail by Schekochihin *et al.* (2002) and more recently the evolution of a 3-D magnetic field by a 2-D flow was examined by Kolokolov (2016). A careful analysis of the time evolving solution indicates that in two dimensions, the energy of any initial magnetic field localized in the wavenumber space will grow exponentially due to the increasing number of excited modes, even if the energy amplitude of each individual mode decreases. This behaviour persists until the length scale of the magnetic field becomes comparable to the dissipation scale, after which dissipation becomes effective and the total magnetic energy decays. The decaying magnetic field spectrum forms a power-law behaviour with an exponent k^2. In contrast in the three-dimensional case for sufficiently large Rm an initial magnetic field localized in space has growing number of excited modes and each mode grows in time. The magnetic energy spectra in 3-D has a power-law $k^{3/2}$ behaviour.

In this paper we are interested in developing the Kazantsev model for a flow where the velocity field takes the form $\boldsymbol{u}=(u(x,y,t),v(x,y,t),w(x,y,t))$, meaning it has three components but depends only on two dimensions. Such flows are referred in the literature as 2.5-D flows. They can be considered as the limiting case of a very fast rotating system for which, according to the Taylor–Proudmann theorem (Proudman 1916; Taylor 1917), the flow becomes two-dimensional due to the Coriolis force that suppresses fluctuations along the direction of rotation. These 2.5-D flows are some of the simplest flows that give rise to the dynamo instability and have been extensively studied for smoothly varying flows (Roberts 1972; Galloway & Proctor 1992). Our interest lies in turbulent flows that have been examined recently at various contexts Smith & Tobias (2004), Tobias & Cattaneo (2008), Seshasayanan & Alexakis (2016) where the dynamo instability driven by a turbulent 2.5-D flow has been studied in detail. In Seshasayanan & Alexakis (2016) it was shown that both helical and non-helical 2.5-D flows can lead to a dynamo instability. For the helical flow and for small Rm the instability can be explained by an α effect. The α effect is a mean field

effect where the small-scale magnetic field and the small-scale velocity field interact to amplify the magnetic fields at large scales. For the non-helical flow however the α coefficient is zero and it does not provide an explanation for the observed dynamo growth rates. Thus this dynamo remains theoretically unexplained.

The main purpose of this work is to examine analytically the dynamo instability for the non-helical flow for the Kazantsev–Kraichnan model of a 2.5-D flow. We first derive a system of equations that govern the second-order correlation function of the magnetic field. This leads to a linear system of equations and an eigenvalue problem which is then solved for a model velocity field that we consider. This allows us to explicitly calculate the growth rate and the spectral behaviour of the most unstable modes. We restrict to the case of smooth velocity fields with a correlation function that scales like r^2 at small scales.

The rest of the article is constructed in the following way. Section 2 describes the governing equations on which this study is based. We set-up a model flow to be studied in § 3. The dynamo instability properties of this model flow are examined in §§ 4 and 5. Section 6 describes the spectral behaviour of the most unstable eigenmode. In § 7, we compare the analytical results with the results from numerical simulations. Finally in § 8 we conclude the study and give some future perspectives.

2. The model

We consider a 2.5-D flow of the form $\boldsymbol{u}(x, y, t) = (u_x, u_y, u_z)$ which can also be written in terms of the streamfunction $\psi(x, y)$ as $\boldsymbol{u} = \boldsymbol{\nabla} \times (\psi \hat{\boldsymbol{e}}_z) + u_z \hat{\boldsymbol{e}}_z = \boldsymbol{u}_{2D} + u_z \hat{\boldsymbol{e}}_z$ where z is the invariant direction. The Kazantsev–Kraichnan ansatz considers the velocity field to be delta correlated in time, Gaussian distributed, its statistics is entirely governed by the second-order correlation function. We further consider that the velocity field is homogeneous and 2-D isotropic in the plane x, y. Isotropy in two dimensions means that the statistics of the velocity field is invariant under rotations around the z-axis. The correlation function of two components of the velocity field u^i, u^j at points $\boldsymbol{x} + \boldsymbol{r}, \boldsymbol{x}$ can be written as,

$$\langle u^i(\boldsymbol{x} + \boldsymbol{r}, t) u^j(\boldsymbol{x}, t') \rangle = g^{ij}(\boldsymbol{r}) \delta(t - t'). \tag{2.1}$$

Independence of g^{ij} on $\boldsymbol{x}$ emerges from homogeneity.

The general form of an isotropic second-order correlation function $g^{ij}(\boldsymbol{r})$ for a 2.5-D flow (see Oughton, Rädler & Matthaeus (1997)) is given by,

$$\begin{aligned} g^{ij}(\boldsymbol{r}) \;=\; & g_{LL}(r)\boldsymbol{\delta}^{ij} - (g_{LL} - g_{NN}) \left(\boldsymbol{\delta}^{ij} - \frac{r^i r^j}{r^2} \right) + (g_Z(r) - g_{2D}(r) - g'_{2D}(r) r) \delta^{i3} \delta^{j3} \\ & + g_c(r) \left(\delta^{i3} \frac{r^j}{r} - \frac{r^i}{r} \delta^{j3} \right) + g_p(r) \left(\boldsymbol{\epsilon}^{3jp} \delta^{i3} \frac{r^p}{r} - \boldsymbol{\epsilon}^{3ip} \delta^{j3} \frac{r^p}{r} \right), \end{aligned} \tag{2.2}$$

where $\boldsymbol{\delta}^{ij}$ is the Kronecker delta tensor and $\boldsymbol{\epsilon}^{ijk}$ is the Levi-Civita tensor. The indices i, j take the values $1, 2, 3$. All the quantities depend only on two dimensions in space, hence we have used a projected coordinate $\boldsymbol{r} = (x, y, 0) = (r^1, r^2, r^3)$ in (2.2). The derivative of $g^{ij}(\boldsymbol{r})$ with respect to $r^3 = z$ is zero. The prime on a scalar function g' denotes the derivative with respect to r. The functions $g_{LL}, g_{NN}, g_c, g_p, g_Z$ are scalar functions that depend only on r and are defined as,

$$\left.\begin{array}{c} g_{LL}(r) = \langle (\boldsymbol{e}_r \cdot \boldsymbol{u})(\boldsymbol{u}' \cdot \boldsymbol{e}_r) \rangle_T, \quad g_Z(r) = \langle (\boldsymbol{e}_z \cdot \boldsymbol{u})(\boldsymbol{u}' \cdot \boldsymbol{e}_z) \rangle_T, \\ g_c(r) = \langle (\boldsymbol{e}_z \cdot \boldsymbol{u})(\boldsymbol{u}' \cdot \boldsymbol{e}_r) \rangle_T, \quad g_p(r) = \langle (\boldsymbol{e}_z \cdot \boldsymbol{u})(\boldsymbol{u}' \cdot (\boldsymbol{e}_z \times \hat{\boldsymbol{r}})) \rangle_T, \\ g_{NN}(r) = \langle ((\boldsymbol{e}_z \times \boldsymbol{e}_r) \cdot \boldsymbol{u})(\boldsymbol{u}' \cdot (\boldsymbol{e}_z \times \boldsymbol{e}_r)) \rangle_T, \end{array}\right\} \tag{2.3}$$

where $\hat{\boldsymbol{r}}$ is the unit vector along $\boldsymbol{r}$ direction. $\boldsymbol{u}$ is the velocity field at a point $\boldsymbol{x}+\boldsymbol{r}$ at time t, $\boldsymbol{u}'$ is the velocity field at a point $\boldsymbol{x}$ at time t', the symbol $\langle\ \rangle_T$ denotes both time average and ensemble average. Physically the quantity g_{LL} measures the longitudinal autocorrelation function of the 2-D velocity field. The quantity g_{NN} gives the transverse autocorrelation of the 2-D velocity field. g_c and g_p are the cross-correlation between the 2-D velocity field and the vertical velocity field. The function g_Z gives the autocorrelation of the vertical velocity field. In particular the function g_p is related to the helicity of the velocity field. Since we consider a velocity field that is non-helical, we take $g_p(r)=0$. The incompressibility condition for the velocity field $\partial_x u_x+\partial_y u_y=0$ implies for the correlation function, $g^{ij}_{,i}=g^{ij}_{,j}=0$, where the subscript $_{,i}$ in $g^{ij}_{,i}$ denotes differentiation of g^{ij} with respect to r^i. This implies,

$$g_{NN}(r)=g_{LL}(r)+g'_{LL}(r)r, \tag{2.4}$$

$$g_c(r)=0, \tag{2.5}$$

leaving two functions $g_{LL}(r)$, $g_Z(r)$ that determine fully the second-order velocity correlation function.

Due to the invariance of the velocity field along z-direction the perturbations of the magnetic field can be decomposed into Fourier modes of the form $\boldsymbol{B}=\boldsymbol{b}(x,y,t)\exp(\mathrm{i}k_z z)$. The complex vector field $\boldsymbol{b}$ is governed by the induction equation which can be written as,

$$\partial_t\boldsymbol{b}+(\boldsymbol{\nabla}\times\psi\hat{\boldsymbol{e}}_z)\cdot\boldsymbol{\nabla}\boldsymbol{b}+u_z\mathrm{i}k_z\boldsymbol{b}=\boldsymbol{b}\cdot\boldsymbol{\nabla}(\boldsymbol{\nabla}\times\psi\hat{e}_z+u_z\hat{e}_z)+\eta(\Delta-k_z^2)\boldsymbol{b}, \tag{2.6}$$

where η is the magnetic diffusivity. The solenoidal condition for the magnetic field $\boldsymbol{\nabla}\cdot\boldsymbol{B}=0$ gives,

$$\partial_x b_x(x,y,t)+\partial_y b_y(x,y,t)=-\mathrm{i}k_z b_z(x,y,t) \tag{2.7}$$

where $\boldsymbol{b}=(b_x,\ b_y,\ b_z)$. The evolution of the magnetic field can be quantified by considering the second-order correlation function defined as,

$$H^{ij}(\boldsymbol{r},t)=\langle(b^i(\boldsymbol{x}+\boldsymbol{r},\boldsymbol{t}))^\dagger b^j(\boldsymbol{x},\boldsymbol{t})\rangle, \tag{2.8}$$

where the symbol † denotes the complex conjugate. As shown in the appendix A, given that the velocity field is mirror symmetric and the governing equation is of the form (2.6), we only need to look at the mirror symmetric part of the magnetic field. This is because the induction equation in the absence of a mirror asymmetric part in the velocity field leads to a decoupled equation for the mirror symmetric and the mirror asymmetric part. Thus we only need to concentrate on the mirror symmetric part of the magnetic field neglecting magnetic helicity similar to most studies of Kazantsev model in 3-D, see however Subramanian (1999), Boldyrev, Cattaneo & Rosner (2005), Malyshkin & Boldyrev (2010), where a helical flow is considered and the magnetic helicity is present. The general form of the magnetic correlation function for a non-helical complex field can be written as,

$$\begin{aligned}H^{ij}(\boldsymbol{r},t)\ =\ & H_{LL}(r)\boldsymbol{\delta}^{ij}-(H_{LL}(r)-H_{NN}(r))\left(\boldsymbol{\delta}^{ij}-\frac{r^i r^j}{r^2}\right)+(H_Z(r)-H_{NN}(r))\delta^{i3}\delta^{j3}\\ &+\mathrm{i}\,H_c(r)\left(\delta^{i3}\frac{r^j}{r}+\frac{r^i}{r}\delta^{j3}\right).\end{aligned} \tag{2.9}$$

where H_{LL}, H_{NN}, H_c, H_Z are scalar real functions that only depend on r and are defined as,

$$\left.\begin{array}{cc} H_{LL}(r,t) = \langle (\boldsymbol{e}_r \cdot \boldsymbol{b}^{\dagger})(\boldsymbol{b}' \cdot \boldsymbol{e}_r)\rangle_T, & H_c(r,t) = \langle (\boldsymbol{e}_z \cdot \boldsymbol{b}^{\dagger})(\boldsymbol{b}' \cdot \boldsymbol{e}_r)\rangle_T, \\ H_{NN}(r,t) = \langle ((\boldsymbol{e}_z \times \boldsymbol{e}_r) \cdot \boldsymbol{b}^{\dagger})(\boldsymbol{b}' \cdot (\boldsymbol{e}_z \times \boldsymbol{e}_r))\rangle_T, & H_Z(r,t) = \langle (\boldsymbol{e}_z \cdot \boldsymbol{b}^{\dagger})(\boldsymbol{b}' \cdot \boldsymbol{e}_z)\rangle_T, \end{array}\right\} \tag{2.10}$$

where $\boldsymbol{b}$ is the magnetic field at a point $\boldsymbol{x}+\boldsymbol{r}$ at time t and $\boldsymbol{b}'$ is the magnetic field at a point $\boldsymbol{x}$ at time t. This general form can be derived by writing the magnetic field in terms of scalar functions and then writing the two point correlation function in terms of these scalar functions (see Oughton *et al.* (1997)). The function H_{LL} is the longitudinal autocorrelation function of the 2-D magnetic field and H_{NN} is the transverse autocorrelation function of the 2-D magnetic field. The function H_c is the cross-correlation function of the 2-D magnetic field with the vertical magnetic field b_z. H_Z is the autocorrelation function of vertical magnetic field b_z. The solenoidal condition of the magnetic field (2.7) for the correlation function implies,

$$H^{ij}_{,i} - \mathrm{i}k_z H^{3j} = 0, \quad H^{ij}_{,j} - \mathrm{i}k_z H^{i3} = 0, \tag{2.11a,b}$$

which gives the set of following relations for the scalar correlation functions,

$$k_z H_Z(\boldsymbol{r}) = H_c'(\boldsymbol{r}) + \frac{H_c(\boldsymbol{r})}{r}, \tag{2.12}$$

$$-k_z H_c(\boldsymbol{r}) = H_{LL}'(\boldsymbol{r}) + \frac{H_{LL}(\boldsymbol{r}) - H_{NN}(\boldsymbol{r})}{r}. \tag{2.13}$$

When $k_z = 0$ we get $H_c = 0$ and $H_{NN} = H_{LL} + rH_{LL}'$. If the magnetic field is 2.5-D, the magnetic correlation function H^{ij} becomes real and it simplifies to a form similar to the velocity correlation function g^{ij}.

Given the velocity correlation functions g^{ij} it is possible to derive the governing equation for H^{ij} starting from the induction equation (2.6). The governing equation for H^{ij} leads to triple product correlations of velocity and magnetic fields. The triple product can be written in terms of second-order correlation functions of the velocity and the magnetic field by using the Furutsu–Novikov theorem (Furutsu 1963; Novikov 1965). This theorem uses the fact that the velocity field is Gaussian distributed. Due to the solenoidal conditions (2.12), (2.13) only two equations are required to completely determine the magnetic correlation function H^{ij} that we here chose to be H_{LL}, H_c. The governing equations then read

$$\begin{aligned} &\partial_t H_{LL} - (2\eta + g_{LL}(0) - g_{LL})\left[H_{LL}'' + 3\frac{H_{LL}'}{r}\right] + k_z^2(2\eta + g_Z(0) - g_Z)H_{LL} = -g_{LL}'' H_{LL} \\ &- g_{LL}'\left(2H_{LL}' + 3\frac{H_{LL}}{r}\right) - 3k_z H_c\, g_{LL}' + \frac{2}{r}(2\eta + g_{LL}(0) - g_{LL})k_z H_c, \end{aligned} \tag{2.14}$$

$$\partial_t H_c - (2\eta + g_{LL}(0) - g_{LL})\left[H_c'' + \frac{1}{r}H_c' - \frac{1}{r^2}H_c\right] + k_z^2(2\eta + g_Z(0) - g_Z)H_c = -k_z g_Z' H_{LL}. \tag{2.15}$$

The details of the derivation are given in the appendix A. The quantity $g_{LL}(0)$ is the total energy of the velocity field in 2-D while the quantity $g_Z(0)$ is the total energy of the velocity in the z direction. These terms, $g_{LL}(0), g_Z(0)$, depend on the frame of reference from which they are measured and do not modify the dynamo instability.

We identify three special cases which do not lead to a dynamo instability.

(i) When $k_z = 0$ the equations simplify to the 2-D Kazantsev model which does not give rise to the dynamo instability as shown in previous studies (see for example Schekochihin *et al.* (2002)). This means that $k_z \neq 0$ is required in order to have a dynamo instability.

(ii) When the third velocity component is zero $u_z = 0$ then $g_Z = 0$. This leads to the function H_c no longer being driven/coupled to H_{LL}. In the presence of diffusivity in the long-time limit H_c would decay to zero. Alternatively we can show that the governing equation for the vertical magnetic field is an advection–diffusion equation without any forcing. Thus the vertical magnetic field b_z decays in the long-time limit. In the absence of H_c the equations governing H_{LL} become again the 2-D Kazantsev equations and hence H_{LL} would also decay in the long time limit.

(iii) The case when there is no shear in the 2-D flow $g_{LL} = g_{LL}(0)$ does not lead to a dynamo instability. The component b_z can be amplified by the stretching of b_x, b_y by u_z. But it can be seen from the induction equation that the magnetic fields components b_x, b_y are advected by u_z and dissipated by the Ohmic dissipation with no amplification from the stretching term. Thus both b_x, b_y decay in the long-time limit which makes b_z to decay in the long-time limit. These special cases fall under the Zeldovich anti-dynamo theorem for 2-D flows. Hence the velocity field has to have all the three components and $k_z \neq 0$ in order for the existence of the dynamo instability in the long-time limit.

In the next section we will consider a model flow where we calculate the form for the functions $g_{LL}(r), g_Z(r)$. We then proceed to study the dynamo instability driven by this model flow in terms of the other control parameters of the system.

3. Model flow

We consider a smooth isotropic and homogeneous velocity field given in terms of the streamfunction ψ and the vertical velocity u_z as,

$$\psi(\boldsymbol{r}, t) = \zeta_1(t) \sin\left(\frac{k_0}{2}[\sin(\phi_1(t))x + \cos(\phi_1(t))y] + \phi_2(t)\right), \tag{3.1}$$

$$u_z(\boldsymbol{r}, t) = \zeta_2(t) \cos\left(\frac{k_0}{2}[\sin(\phi_1(t))x + \cos(\phi_1(t))y] + \phi_2(t)\right). \tag{3.2}$$

$\phi_1(t)$, $\phi_2(t)$ are random variables which are uniformly distributed over $[0, 2\pi]$ and render the flow homogeneous and isotropic. $\zeta_1(t)$ and $\zeta_2(t)$ are random variables that are Gaussian distributed in time with $\langle \zeta_1(t)\zeta_1(t')\rangle = \Theta_1 \delta(t - t')$, $\langle \zeta_2(t)\zeta_2(t')\rangle = \Theta_2 \delta(t - t')$ and $\langle \zeta_1(t)\zeta_2(t')\rangle = 0$. The wavenumber k_0 defines a typical length scale for the velocity field. This is a simple single wavenumber flow that is both isotropic and homogeneous. The correlation function of the velocity field is calculated to be,

$$g^{ij}(\boldsymbol{r}) = \frac{k_0\Theta_1}{4}\left\{-\boldsymbol{\delta}^{ij}\frac{\mathrm{J}_0'\left(k_0\frac{r}{2}\right)}{r} + \left(\boldsymbol{\delta}^{ij} - \frac{r^i r^j}{r^2}\right)\left(\frac{\mathrm{J}_0'\left(k_0\frac{r}{2}\right)}{r} - \frac{k_0}{2}\mathrm{J}_0''\left(k_0\frac{r}{2}\right)\right)\right\} + \frac{\Theta_2}{2}\mathrm{J}_0\left(k_0\frac{r}{2}\right)\delta^{i3}\delta^{j3}, \tag{3.3}$$

where J_0 is the Bessel function of the first kind and J_0' stands for its derivative. The functions g_{2D}, g_Z are then,

$$g_{2D}(r) = -\frac{k_0\Theta_1}{4r} J_0'\left(k_0\frac{r}{2}\right), \quad g_Z(r) = \frac{\Theta_2}{2} J_0\left(k_0\frac{r}{2}\right). \tag{3.4a,b}$$

The small r behaviour of these functions is,

$$g_{2D}(r) = g_{2D}(0) - D_1 r^2 + E_1 r^4 - O(r^6), \quad g_Z(r) = g_Z(0) - D_2 r^2 + E_2 r^4 - O(r^6), \tag{3.5a,b}$$

where $g_{2D}(0) = k_0^2\Theta_1/16$, $g_Z(0) = \Theta_2/2$, $D_1 = k_0^4\Theta_1/512$, $D_2 = k_0^2\Theta_2/32$. At small scales the velocity field is smooth and behaves like $g_{2D} \sim r^2$, $g_Z \sim r^2$.

We note that D_1 has dimensions of inverse time and defines the dynamical time scale $\tau_d \equiv 1/D_1$ that we will use to non-dimensionalize our system. Accordingly the magnetic Reynolds number is defined as the ratio of the diffusion time scale $1/\eta k_0^2$ to the dynamical time scale $Rm \equiv D_1/(k_0^2\eta) = k_d^2/k_0^2$ where k_d is the dissipation length scale for the magnetic field $k_d \equiv k_0\sqrt{D_1/\eta} = k_0\sqrt{Rm}$. A third dimensionless parameter can be defined by the ratio of the vertical velocity field gradients to the planar velocity field gradients that we will quantify as $D_r = D_2/D_1$. The quantity D_r depends on the ratio of the amplitudes of $k_0^2\Theta_1$ and Θ_2 given as $D_r = 16\Theta_2/(\Theta_1 k_0^2)$. Thus the non-dimensionalized control parameters are, the wavemode k_z/k_0, the magnetic Reynolds number Rm and D_r.

4. Growth rate γ

Substituting $H_{LL} = e^{\gamma t} h_{LL}$ and $H_c = e^{\gamma t} h_c$ in (2.15) we end up with an eigenvalue problem for the growth rate of the magnetic energy γ and the eigenfunctions h_{LL} and h_c. The boundary conditions are $h_{LL}'(0) = 0$, $h_c(0) = 0$, $h_{LL}(\infty) = 0$, $h_c(\infty) = 0$. The largest eigenvalue of the system γ controls the long-time evolution of the magnetic field correlation functions. We note that since H_{LL} and H_c are quadratic quantities in the magnetic field $\boldsymbol{b}$ the growth rate γ is twice the growth rate of the magnetic field. We proceed in this section by solving the resulting system of equations numerically. To solve the eigenvalue problem we use a Chebyshev spectral method to discretize the domain $[0, r_{max}]$, and we project the functions $h_{LL}(r)$, $h_c(r)$, $g_{LL}(r)$, $g_Z(r)$ into a truncated basis of Chebyshev functions. The equations (2.15) in this truncated basis can now be reduced to a linear matrix eigenvalue problem. We compute the largest positive eigenvalue of the discretized matrix using standard linear algebra software. We have checked the convergence of the resulting eigenvalue in terms of the number of basis functions used and the domain size r_{max}.

Figure 1 shows the growth rate γ as a function of the rescaled parameter k_z/k_d for different values of Rm. Dynamo instability appears at values of Rm above the critical magnetic Reynolds number Rm_c which is found to be $Rm_c \approx 0.45$. Close to Rm_c the instability occurs at the value $k_z \approx 0.18 k_d \approx 0.12 k_0$. For larger values of Rm the instability is found in a range of wavenumbers $k_{min} < k < k_{max}$. The maximum value of k_z/k_d at which the dynamo instability occurs initially increases with Rm but reaches a constant value independent of Rm for large value of Rm. We note that $k_d \propto k_0\sqrt{Rm}$ thus the largest wavenumber k_{max} for which there is a dynamo instability increases like $k_{max} \sim k_0\sqrt{Rm}$. The smallest wavenumber at which dynamo instability occurs k_{min} decreases as we increase Rm. The growth rate of each mode k_z increases as we increase Rm reaching an asymptotic value at large Rm. The supreme of the growth rate $\gamma\tau_d = 3$ is obtained for $Rm \to \infty$ and $k_z \to 0$. For very large Rm we see that the curves themselves seem to reach an asymptotic behaviour which is captured well by the black solid curve representing the growth rate in the limit of $Rm \to \infty$ that we discuss in the next section.

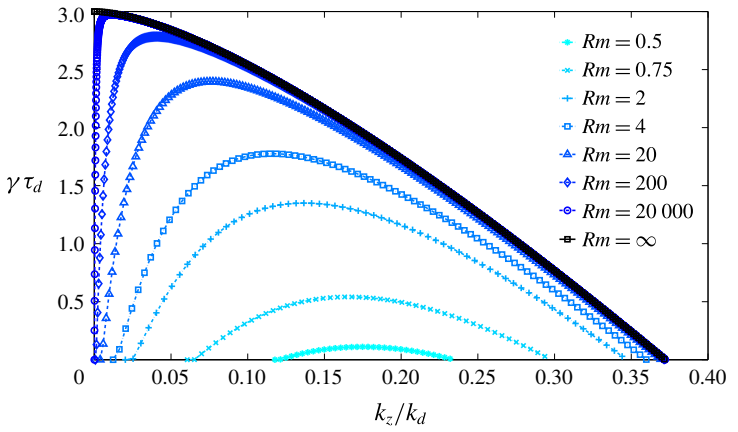

FIGURE 1. (Colour online) Normalized growth rate $\gamma\tau_d$ is shown as a function of the normalized modes k_z/k_d for different values of Rm. Darker shades correspond to larger values of Rm.

5. Three limiting behaviours

In this section we look at three different limits of the control parameters.

5.1. $Rm \to \infty, k_z \to 0$

The limit of very large Rm can be taken by letting the quantity $\eta \to 0$ in the (2.15). In this limiting procedure we do the following change of variables, $\tilde{r} = r\,k_d$, $\tilde{t} = t\eta k_d^2 = t/D_1$. The velocity correlation functions are expanded in the following way, $g_{2D}(\tilde{r}) = g_{2D}(0) - \eta\tilde{r}^2 + O(\eta^2\tilde{r}^4)$, $g_Z = g_Z(0) - D_r\eta\tilde{r}^2 + O(\eta^2\tilde{r}^4)$. Simplifying the resulting equation by considering only the lowest-order terms in η we get,

$$\gamma\tau_d h_{LL} - (2+\tilde{r}^2)\left[h''_{LL} + 3\frac{h'_{LL}}{\tilde{r}}\right] + \tilde{k}_z^2(2+D_r\tilde{r}^2)h_{LL} = 2h_{LL} + 2\tilde{r}\left(2h'_{LL} + 3\frac{h_{LL}}{\tilde{r}}\right) + 6\tilde{r}\tilde{k}_z h_c + \frac{2}{\tilde{r}}(2+\tilde{r}^2)\tilde{k}_z h_c, \tag{5.1}$$

$$\gamma\tau_d h_c - (2+\tilde{r}^2)\left[h''_c + \frac{1}{\tilde{r}}h'_c - \frac{1}{\tilde{r}^2}h_c\right] + \tilde{k}_z^2(2+D_r\tilde{r}^2)h_c = 2\tilde{k}_z D_r\tilde{r}h_{LL}. \tag{5.2}$$

Note that in this limit the growth rate does not depend on k_0 or the exact form of the flow but only on the local structure of the velocity field described by D_r. The eigenvalues of the black solid curve in figure 1 were obtained by solving the above set of equations. It is important to note that the above set of equations are obtained in the limit of $\eta \to 0$ and not the case of $\eta = 0$. We find that the value of $\gamma(k_z \to 0) = 3$ as $Rm \to \infty$. This value can be obtained by a matched asymptotic expansion that is described in § 6 and in appendix D. On the other hand, for a finite Rm we see that $\gamma(k_z \to 0) = 0$. Thus we have the non-commuting limits,

$$3 = \lim_{k_z\to 0}\lim_{Rm\to\infty}\gamma \neq \lim_{Rm\to\infty}\lim_{k_z\to 0}\gamma = 0. \tag{5.3}$$

We mention here that the anti-dynamo theorem is still respected since it corresponds to the second limiting procedure above.

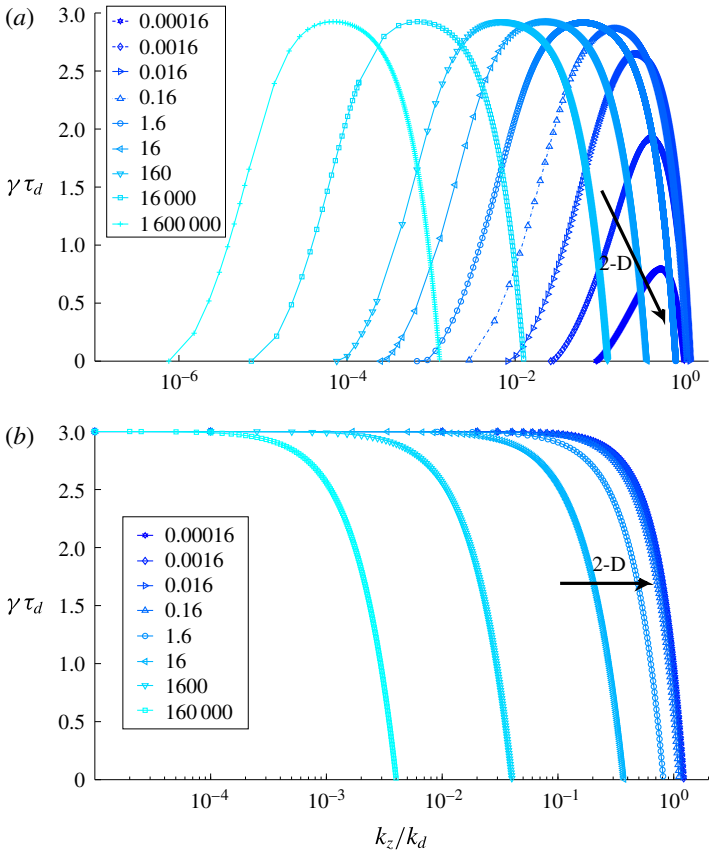

FIGURE 2. (Colour online) Normalized growth rate γ as a function of k_z/k_d for different values of D_r mentioned in the legends for, (*a*) a finite $Rm \approx 1.95 \times 10^5$, (*b*) the case $Rm \to \infty$. The black arrow marked 2-D shows the direction of decreasing value of the parameter D_r. Darker shades correspond to smaller values of D_r.

5.2. $Rm \to \infty$, $D_r \to 0$

Taking the limit $D_r \to 0$ reduces the flow to a 2-D flow and from the anti-dynamo theorem we expect the dynamo instability to disappear. In figure 2 we show γ as a function of k_z/k_d for a finite Rm case on the top and for the case of $Rm \to \infty$ on the bottom for different values of the parameter D_r as mentioned in the respective legends. The growth rate γ and the range of unstable modes k_z depend on the value of D_r. In figure 2(*a*) we see that indeed for the finite Rm case as D_r is decreased the dynamo instability disappears. This limit is pointed out in the plot by the arrow marked 2-D. On the contrary for the case of the $Rm \to \infty$ (see figure 2*b*) the growth rate γ curve reaches a non-zero asymptotic behaviour as $D_r \to 0$ marked in the figure by the arrow marked 2-D. Thus we obtain another set of non-commuting limits,

$$0 < \lim_{D_r \to 0} \lim_{Rm \to \infty} \gamma \neq \lim_{Rm \to \infty} \lim_{D_r \to 0} \gamma = 0. \tag{5.4}$$

This result needs to be explained. The case of $D_r = 0$ is a purely 2-D flow and does not give rise to the dynamo instability in accordance with the anti-dynamo theorem

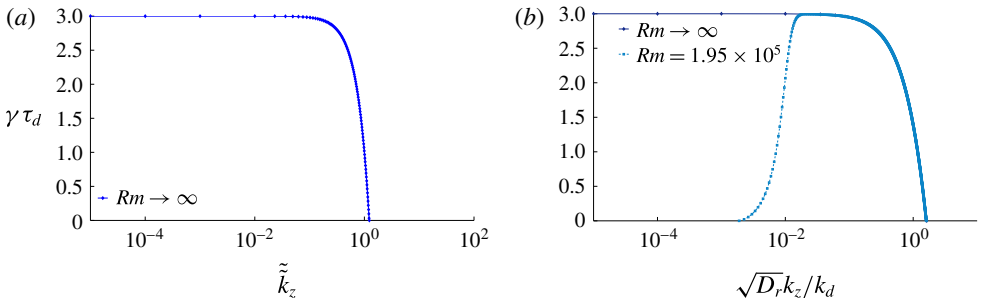

FIGURE 3. (Colour online) Growth rate as a function of the rescaled k_z for the case of, (*a*) the limit $D_r \to 0$ where only the infinite Rm has a dynamo effect and (*b*) the limit $D_r \to \infty$ where both the finite and the infinite Rm have dynamo instability.

which is respected by the governing equations. We can capture the limit of $D_r \to 0$ taken after the limit $Rm \to \infty$ by applying the following rescaling, $\sqrt{D_r}\tilde{r} \to \tilde{\tilde{r}}$, $h_c \to \sqrt{D_r}\tilde{h}_c$ to (5.2). The lowest order in D_r which captures the limit $D_r \to 0$ leads to the following set of equations,

$$\gamma\tau_d h_{LL} - \tilde{\tilde{r}}^2\left[h''_{LL} + 3\frac{h'_{LL}}{\tilde{\tilde{r}}}\right] + k_z^2(2+\tilde{\tilde{r}}^2)h_{LL} = 2h_{LL} + 2\tilde{\tilde{r}}\left(2h'_{LL} + 3\frac{h_{LL}}{\tilde{\tilde{r}}}\right) + 8\tilde{\tilde{r}}k_z\tilde{h}_c, \tag{5.5}$$

$$\gamma\tau_d\tilde{h}_c - \tilde{\tilde{r}}^2\left[\tilde{h}''_c + \frac{1}{\tilde{\tilde{r}}}\tilde{h}'_c - \frac{1}{\tilde{\tilde{r}}^2}\tilde{h}_c\right] + k_z^2(2+\tilde{\tilde{r}}^2)\tilde{h}_c = 2k_z\tilde{\tilde{r}}h_{LL}. \tag{5.6}$$

The eigenvalues of these equations give the asymptotic behaviour of the growth rate when first the limit $Rm \to \infty$ is taken and then the limit $D_r \to 0$. The resulting eigenvalues from the above set of equations are shown separately in figure 3(*a*). These results are valid provided that $1 \gg D_r \gg Rm^{-1}$, but the expansion fails if D_r is the same order as Rm^{-1}. For values of D_r smaller than this threshold the dissipation effects are stronger and the dynamo instability disappears.

5.3. $Rm \to \infty, D_r \to \infty$

In figure 2(*a*) as the parameter $D_r \to \infty$ we see that the unstable k_z modes move towards smaller values. This implies that the magnetic field should be correlated over longer distances along the z direction in order for a large u_z to twist and fold the field lines and result in the amplification of the magnetic field. A similar behaviour is observed in the case of infinite Rm ($Rm \to \infty$), shown in figure 2(*b*). It is important to note here that the growth rate γ is non-dimensionalized with D_1 which is related to the amplitude of the shear in the correlation function g_{2D}. If the growth rate is normalized with $\sqrt{D_1^2 + D_2^2}$ which takes into account both the shear in u_{2D} and u_z then the normalized growth rate $\gamma/\sqrt{D_1^2+D_2^2} = \gamma\tau_d/\sqrt{1+D_r^2}$ becomes zero in the limit $D_r \to \infty$. In this limit there is no violation of the anti-dynamo theorem. The maximum growth rate in figure 2 appears to be independent of D_r in the large D_r limit. The growth rate curves for large D_r can be plotted with a rescaled $k_z \to \sqrt{D_r}k_z$ which makes the curves collapse onto each other (not shown here). Such a result can

be obtained by expanding the (2.15) in terms of $1/D_r$ and solving for the lowest-order equations which represents the limit $D_r \to \infty$. Since the steps are similar with the previous section the resulting set of equations are not shown.

The eigenvalues of the resulting equations after taking the limit $D_r \to \infty$ are shown in figure 3(*b*). In this plot we show both the finite *Rm* and the infinite *Rm* growth rates. The behaviour of the two curves are similar except for the small k_z where the finite *Rm* limit looses the dynamo instability as shown in § 5.1. For fixed k_z/k_d, however, the limits $\lim_{Rm\to\infty}$ and $\lim_{D_r\to\infty}$ are commuting:

$$\lim_{Rm\to\infty}\lim_{D_r\to\infty}\gamma = \lim_{D_r\to\infty}\lim_{Rm\to\infty}\gamma. \tag{5.7}$$

6. Correlation functions and energy spectra

In this section we discuss the functional form of the correlation functions and the spectra of the most unstable eigenmode. It is reminded that the magnetic energy spectra of a magnetic field advected by a Kazantsev 2-D flow show the power-law behaviour k^2 for wavenumbers between the velocity wavenumber k_0 and the dissipation wavenumber k_d. While in 3-D the spectrum of the unstable mode scales like $k^{3/2}$ in the same range. For the 2.5-D problem there are 3 relevant scales k_z, k_d, k_0. Dynamo instability is obtained only for a particular ordering of these scales. Based on the results from the previous sections, to obtain a dynamo $\sqrt{D_r}k_z$ cannot be much larger than k_d nor much smaller than k_0, more precisely $c_{min}k_0 \leqslant \sqrt{D_r}k_z < c_{max}k_d$. The two constants c_{min} and c_{max} are related to k_{min} and k_{max} respectively discussed in § 4. It is found that c_{min} depends on the *Rm* and $c_{max} \approx 1.6$ calculated for large *Rm*. We concentrate on the case of $Rm \to \infty$ where we have two scales in the system k_d, k_z. First we examine the behaviour of the correlation functions $h_{LL}(r), h_c(r)$ before moving to the spectra of the magnetic field.

We start with (5.2), for $Rm \to \infty$ where the equations are written in terms of the rescaled quantities $\tilde{r}, \tilde{k}_z$. The dissipation scale $r_d = 1/k_d$ is given by $\tilde{r} = 1$. The small and large $\tilde{r}$ asymptotics of $h_{LL}(\tilde{r}), h_c(\tilde{r})$ are mentioned in appendix B. There are three distinct range of scales that display different behaviour. The small $\tilde{r}$ corresponds to the regime of scales below the dissipation scale $\tilde{r} \ll 1$, the large $\tilde{r}$ corresponds to the regime $\tilde{r} \gg 1/\tilde{k}_z$. In between these two range of scales we have an intermediate range of scales $1 \ll \tilde{r} \ll 1/k_z$. The scaling in this range of scales can be obtained by using matched asymptotics, the details of which are given in the appendix D. In this process we also find that in the limit of $\tilde{k}_z \to 0$ we can obtain the eigenvalue $\gamma \to 3$ independent of the value of D_r, in accordance with results shown in figures 1 and 2. The correlation functions $h_{LL}(r), h_c(r)$ show the following scaling with the variable r for the large *Rm* limit,

$$h_{LL} = \begin{cases} 1 - c_1 r^2 + O(r^4) & \text{if } r \ll \dfrac{1}{k_d}, \\ c_2 r^{-1} & \text{if } \dfrac{1}{k_d} \ll r \ll \dfrac{1}{k_z}, \\ \mathrm{e}^{-c_3 r} & \text{if } r \gg \dfrac{1}{k_z}, \end{cases} \quad h_c = \begin{cases} c_4 r^1 & \text{if } r \ll \dfrac{1}{k_d}, \\ c_5 r^0 & \text{if } \dfrac{1}{k_d} \ll r \ll \dfrac{1}{k_z}, \\ \mathrm{e}^{-c_2 r} & \text{if } r \gg \dfrac{1}{k_z}, \end{cases} \tag{6.1a,b}$$

where c_1, c_2, c_3, c_4, c_5 are related to η, k_z, D_r and can be found from the calculation in appendix D. In figure 4 we show the correlation functions $h_{LL}(\tilde{r}), h_c(\tilde{r})$ for $\tilde{k}_z = 0.005$, $D_r = 1$. Since the equations are rescaled with k_d the dissipation scale is given

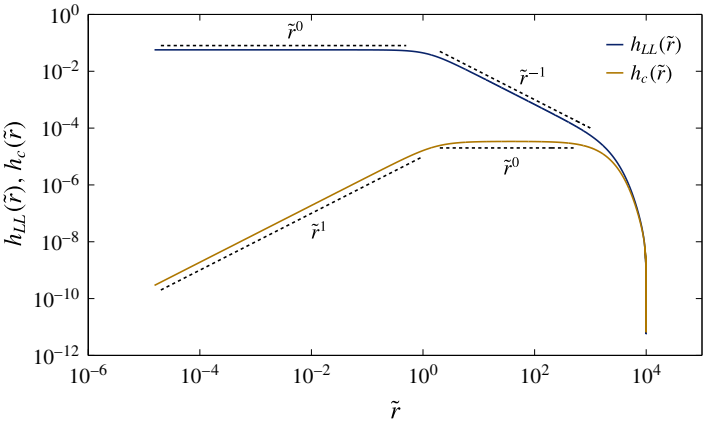

FIGURE 4. (Colour online) The correlation functions of the magnetic field $h_{LL}(\tilde{r})$ in dark blue, $h_c(\tilde{r})$ in light brown for $k_z = 0.005$ with $D_r = 1$. The black dashed lines denote exponents that are observed in the respective range of scales.

by $\tilde{r} = 1$. We can see that the behaviour of the functions $h_{LL}(\tilde{r})$, $h_c(\tilde{r})$ described in (6.1) is well captured from the numerics.

Now with the solution of $h_{LL}(r)$, $h_c(r)$ we can construct the spectra using the Wiener–Khinctine relation (see Chatfield (1989)) in two dimensions. For a function $M(r)$ its isotopic Fourier spectrum reads as,

$$\widehat{M}(k) = k \int_0^\infty rM(r)\mathrm{J}_0(kr)\,\mathrm{d}r. \tag{6.2}$$

For the magnetic field we can construct the planar magnetic field spectrum $E^B_{2D}(k)$ and the vertical magnetic energy spectrum $E^B_Z(k)$. Their relations with $h_{LL}(r)$, $h_c(r)$ are given by,

$$E^B_{2D}(k) = k \int_0^\infty r(2h_{LL}(r) + rh'_{LL}(r) + rk_z h_c(r))\mathrm{J}_0(kr)\,\mathrm{d}r, \tag{6.3}$$

$$E^B_Z(k) = k \int_0^\infty r\frac{1}{k_z}\left(h'_c(r) + \frac{h_c(r)}{r}\right)\mathrm{J}_0(kr)\,\mathrm{d}r. \tag{6.4}$$

Using the behaviour of the correlation functions $h_{LL}(r)$, $h_c(r)$ mentioned in (6.1) we can use the Wiener–Khintchine relation to get the behaviour of $E^B_{2D}(k)$, $E^B_Z(k)$ in the regimes $k \ll k_z$, $k_z \ll k \ll k_d$, $k \gg k_d$. We can write the generalized spectra of the magnetic field in the limit of large-scale separation $k_z \ll k_d$ as,

$$E^B_{2D}(k) = \begin{cases} k^1 & \text{if } k \ll k_z, \\ k^0 & \text{if } k_z \ll k \ll k_d, \\ \mathrm{e}^{-k/k_d} & \text{if } k \gg k_d, \end{cases} \quad E^B_Z(k) = \begin{cases} k^3 & \text{if } k \ll k_z, \\ k^0 & \text{if } k_z \ll k \ll k_d, \\ \mathrm{e}^{-k/k_d} & \text{if } k \gg k_d. \end{cases} \tag{6.5a,b}$$

These predicted power laws are in agreement with the solutions of the (5.2) displayed in figure 5. In this figure the dissipation wavenumber is unity and k_z is varied with the values mentioned in the legend. Figure 6 summarizes the form of the unstable mode for the different range of scales in both k and r for the case of large-scale separation $k_z \ll k_d$ and generalized to take into account the variation in D_r.

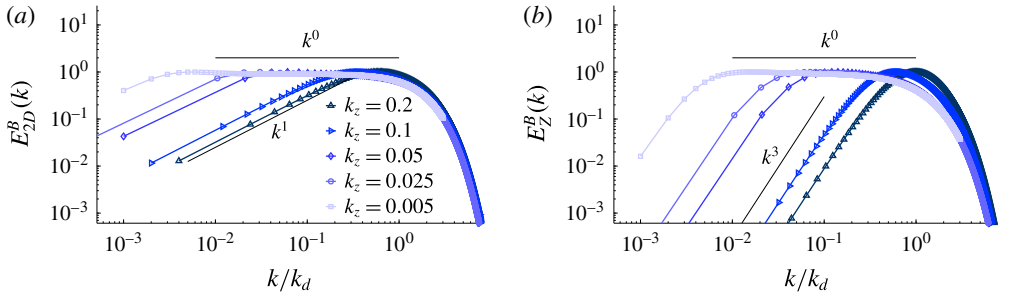

FIGURE 5. (Colour online) Spectra of the magnetic field, (*a*) $E^B_{2D}(k)$, and (*b*) $E^B_Z(k)$, for different values of k_z shown in the legends. Lighter shades of blue correspond to smaller values of k_z. The parameter $D_r = 1$, the black lines denote power laws.

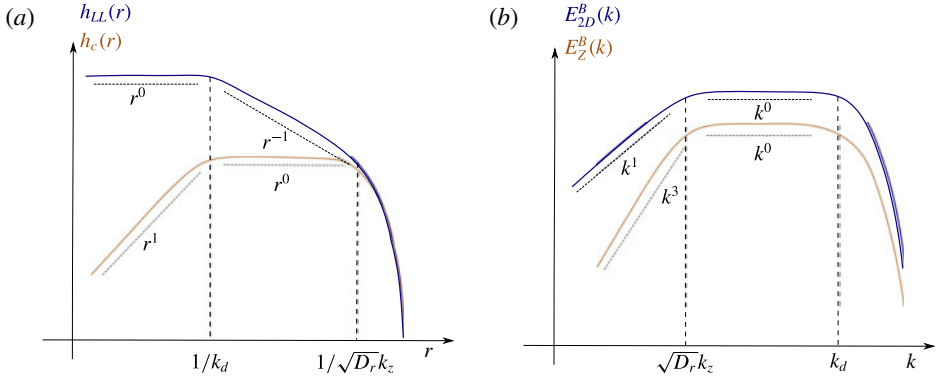

FIGURE 6. (Colour online) The form, (*a*) of the correlation functions $h_{LL}(r)$ in a dark shade of blue, $h_c(r)$ in a light shade brown and (*b*) the spectra $E^B_{2D}(k)$ in a dark shade of blue, $E^B_Z(k)$ in a light shade brown. The black dashed lines represent the different exponents which are observed in the respective range of scales.

7. Comparison with direct numerical simulations

7.1. *White noise flows*

In order to test the relevance of the theoretical results with the results of direct numerical simulations (DNS) we consider and solve numerically the partial differential equation (2.6) for a random Gaussian distributed flow in a finite 2-D periodic box. We note that the 2-D periodic flow does not respect isotropy. This is true for any finite homogeneous system, thus we will be limited to only a qualitative comparison. We consider a random flow of the form,

$$\psi(x, y, t) = \zeta_3(t)[\sin(\phi_3(t))\cos(k_f x + \phi_4(t)) + \cos(\phi_3(t))\sin(k_f y + \phi_4(t))]/k_f, \quad (7.1)$$

$$u_z(x, y, t) = \zeta_4(t)[\sin(\phi_3(t))\sin(k_f x + \phi_4(t)) + \cos(\phi_3(t))\cos(k_f y + \phi_4(t))], \quad (7.2)$$

where $\zeta_3(t)$, $\zeta_4(t)$ are two Gaussian distributed random variables satisfying the relations, $\langle\zeta_3(t)\zeta_3(t')\rangle = \delta(t - t')$, $\langle\zeta_4(t)\zeta_4(t')\rangle = \delta(t - t')$, $\langle\zeta_3(t)\zeta_4(t')\rangle = 0$. $\phi_3(t)$, $\phi_4(t)$ are uniformly distributed random variables in the interval $[0, 2\pi]$. The above flow is realized in a domain $[2\pi L, 2\pi L]$ with $k_f L$ being the forcing wavenumber. The above system is homogeneous and invariant under $\pi/2$ rotations. The discretized

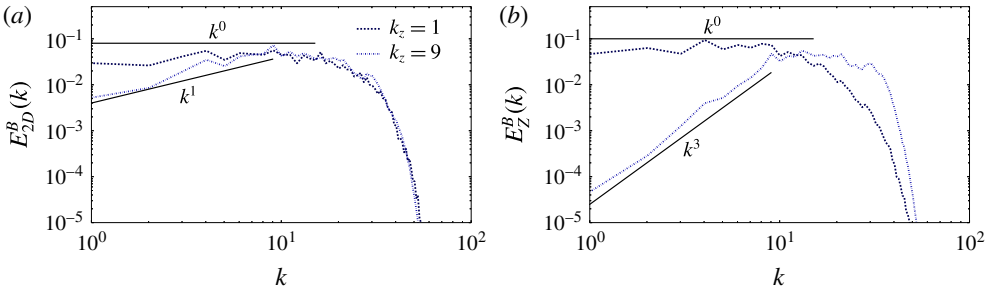

FIGURE 7. (Colour online) The magnetic field spectrum at one instant of time with E^B_{2D} (a) and E^B_Z (b), for two values of k_z mentioned in the legend, lighter shades correspond to increasing values of k_z. The results correspond to the fluctuating velocity field with parameters $Rm \approx 460$.

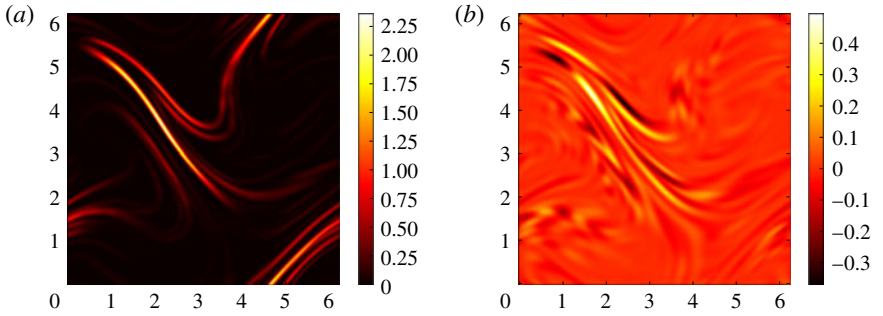

FIGURE 8. (Colour online) The contour of the magnetic field with $|\boldsymbol{b}_{2D}|^2$ in (a) and the real part of b_z in (b). The results correspond to the fluctuating velocity field with parameters $Rm \approx 210$ and $k_z/k_d \approx 0.35$.

version of the induction equation is numerically solved with the realization of the noise changing at each time step with the Stratonovich formulation of the noise (see Greiner, Strittmatter & Honerkamp (1988), Leprovost (2004)).

The growth rate calculated for the magnetic field with $k_f = 1$ is shown in figure 9(a) for a few values of Rm. Qualitatively the results reproduce the behaviour of the theoretical predictions. The spectra of the growing magnetic field are shown in figure 7 for a single time realizations for a $Rm \approx 460$ and two values of k_z mentioned in the legend. The theoretical predictions are shown in black solid lines and they compare well with the numerical results. The magnetic field intensity is shown in figure 8, where (a) shows $|\boldsymbol{b}_{2D}|^2 = b_x^\dagger b_x + b_y^\dagger b_y$ the magnetic energy in the 2-D plane and (b) shows the real part of the vertical magnetic field b_z. The magnetic field lines are concentrated in thin filamentary structures and their size decreases as Rm is increased.

7.2. *Freely evolving flows*

To test the validity of the model for more realistic flows we also compare our results with the growth rates of freely evolving chaotic/turbulent flows. We consider a flow driven by a non-helical forcing at a wavenumber $k_f = 4$ that is constant in time. The temporal behaviour of the flow and its 'randomness' originates purely from the chaotic

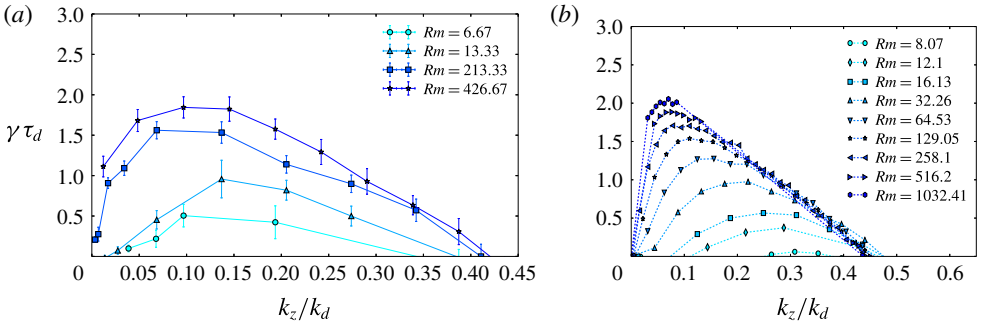

FIGURE 9. (Colour online) The growth rate γ as a function of the normalized wavemode k_z/k_d for, (*a*) the delta correlated flow and (*b*) for a time correlated flow. Darker shades correspond to larger values of Rm.

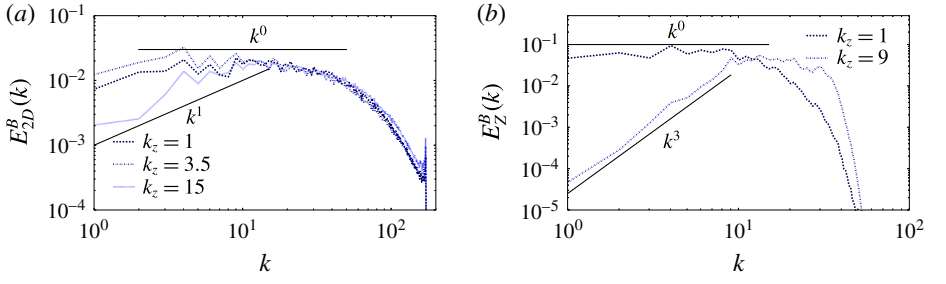

FIGURE 10. (Colour online) A time shot of the magnetic field spectra E^B_{2D} (*a*) and E^B_Z (*b*) for a few different values of k_z mentioned in the legend. Lighter shades correspond to increasing values of k_z. The results correspond to the kinematic dynamo problem of the forced Navier–Stokes equation with parameters $Rm \approx 1020$, $Re \approx 32$.

dynamics of the Navier–Stokes equation. The details of the full study of this system of equations can be found in Seshasayanan & Alexakis (2016).

The normalized growth rate γ obtained from the turbulent flow is shown in figure 9(*b*) as a function of the normalized k_z/k_d and for different values of Rm. For the examined flow the quantity $k_d = k_f\sqrt{Rm}$ and $Rm = u/(k_f\eta)$, $\tau_d = 1/(\eta k_d^2)$ where u is the root-mean-square velocity. We find a good match in terms of the behaviour of the growth rates and its dependence on k_z/k_d, Rm. The spectra of the magnetic field, E^B_{2D} and E^B_Z are also shown in figure 10 along with the black solid lines denoting the theoretical prediction mentioned in the previous section. The spectra shown correspond to a simulation run with the parameters $Rm \approx 1020$, $Re \approx 32$ taken after $t \approx 100$ nonlinear time scales. The theoretical predictions seem to capture well the shape of the unstable spectra.

8. Conclusions

In this work we have examined the dynamo properties of the Kazantsev–Kraichnan model for 2.5-D flows. The simplicity of the model allowed us to examine analytically and in detail various limits of the system. In particular we were able to examine the dynamo properties of the system when the system is close to certain classes of flows that dynamo action is 'forbidden' by the Zeldovich anti-dynamo theorem. In particular

our results showed that the limits $k_z \to 0$ and $D_r \to 0$ (that correspond to 2-D magnetic fields and 2-D velocity fields respectably) do not commute with $Rm \to \infty$ limit. This implies that the large Rm results are valid provided that $Rm \gg 1/D_r$, and $Rm \gg k_0/k_z$ and not for the exactly 2-D case.

Our analysis also allowed us to predict the functional form of the energy spectra of the unstable dynamo modes. Two power-law behaviours were predicted. In the range of wavenumbers $k_0 \ll k \ll k_z$ the magnetic energy spectra satisfy $E^B_{2D} \propto k^1$ and $E^B_Z \propto k^3$ while in the range $k_z \ll k \ll k_d$ the spectra satisfy $E^B_{2D} \propto E^B_Z \propto k^0$. A summary of this behaviour is depicted in figure 6. These predictions are new and cannot be obtained simply by dimensional analysis.

Finally we compared the theoretical results to direct numerical simulation of homogeneous, delta-correlated, Gaussian distributed flow and freely evolving flows based on the Navier–Stokes equations. In both the cases the growth rate curves matched qualitatively with the model and the magnetic field spectra are in agreement with the theoretical predicted power laws. This gives support in the relevance of these results to more realistic flows that might occur in nature.

Our study was limited only for smooth non-helical flows at high magnetic Prandtl numbers. In realistic fast rotating systems driven by convection, one must take into considerations kinetic helicity possibly injected by the forcing or from the effect of boundaries. Another interesting extension would be to study the dynamo instability driven by rough flows that resembles the turbulent scales under fast rotation and correspond to low magnetic Prandtl number flows. For the rough flows the Hölder exponent ζ for the second-order correlation function of the velocity field should take into account the Kolmogorov spectra of 2-D turbulence. This leads to very interesting possibilities. For scales smaller than the forcing scale the 2-D velocity field $\boldsymbol{u}_{2D}$ forms a k^{-3} energy spectrum and would continue to follow the r^2 scaling for g_{2D}. However the vertical velocity field that is advected like a passive scalar and has a spectrum proportional to k^{-1} would have $g_Z \propto r^0$ scaling with possible logarithmic corrections. For scales larger than the forcing scale an inverse energy cascade develops with a Kolmogorov energy spectrum $k^{-5/3}$ for $\boldsymbol{u}_{2D}$ while u_z reaches a thermalized distribution k^1. This implies that the correlation function g_{2D} will follow a $r^{2/3}$ scaling while the vertical scales will have a much shallower scaling. We plan to address these possibilities in our future work.

Acknowledgements

The authors would like to thank the group of S. Fauve for their very useful comments and fruitful discussions. K.S. would like to thank R. V. K. Chakravarthy for his help in resolving the eigenvalue problem. The present work benefited from the computational support of the HPC resources of GENCI-TGCC-CURIE & GENCI-CINES-JADE (Project Nos x2014056421 and x2015056421) and MesoPSL financed by the Region Ile de France and the project EquipMeso (reference ANR-10-EQPX-29-01) where the numerical simulations have been performed.

Appendix A. Derivation of the equations

In order to derive the (2.15) we follow a procedure similar to the one mentioned in Schekochihin *et al.* (2002). We start with the index form of the induction equation (2.6) written as,

$$\partial_t b^i = b^m \partial^m u^i - u^m \partial^m b^i - \mathrm{i}\, k_z\, u_z b^i + \eta(\partial^k \partial^k - k_z^2) b^i, \tag{A 1}$$

where ∂^i denotes the derivative with respect to the coordinate x^i. Next we write the equation for the magnetic correlation function $H^{ij}(\boldsymbol{r}) = \langle (b^i(\boldsymbol{x}+\boldsymbol{r}))^\dagger b^j(\boldsymbol{x})\rangle$, which reads as,

$$\begin{aligned}\partial_t H^{ij} - 2\eta(\Delta - k_z^2)H^{ij} &= \partial_k[C^{ikj}(\boldsymbol{r},t) - C^{kij}(\boldsymbol{r},t) - (C^{jki}(-\boldsymbol{r},t))^\dagger + (C^{kji}(-\boldsymbol{r},t))^\dagger] \\ &+ \mathrm{i}k_z[C^{3ij}(\boldsymbol{r},t) - (C^{3ji}(-\boldsymbol{r},t))^\dagger - C^{i3j}(\boldsymbol{r},t) + (C^{j3i}(-\boldsymbol{r},t))^\dagger], \end{aligned} \tag{A 2}$$

where the quantity C^{kij} is the triple product average defined as $C^{kij}(\boldsymbol{r},t) = \langle u^k(\boldsymbol{x}+\boldsymbol{r},t)(b^i(\boldsymbol{x}+\boldsymbol{r},t))^\dagger b^j(\boldsymbol{x},t)\rangle$. This triple product average can be simplified using the Furutsu–Novikov theorem which can be written as,

$$\begin{aligned} C^{kij}(\boldsymbol{r},t) &= \langle u^k(\boldsymbol{x}+\boldsymbol{r},t)(b^i(\boldsymbol{x}+\boldsymbol{r},t))^\dagger b^j(\boldsymbol{x},t)\rangle \\ &= \int \mathrm{d}x'\,\mathrm{d}t' \langle u^k(\boldsymbol{x}+\boldsymbol{r},t)u^m(\boldsymbol{x}',t')\rangle \left\langle \frac{\delta((b^i(\boldsymbol{x}+\boldsymbol{r},t))^\dagger b^j(\boldsymbol{x},t))}{\delta u^m(\boldsymbol{x}',t')}\right\rangle. \end{aligned} \tag{A 3}$$

The above expression can be simplified by using the delta-correlation property of the velocity correlator. The term $\langle(\delta((b^i(\boldsymbol{x}+\boldsymbol{r},t))^\dagger b^j(\boldsymbol{x},t)))/(\delta u^m(\boldsymbol{x}',t'))\rangle$ can be simplified by taking the functional derivative of the governing equation of the two point magnetic correlation function $(b^i)^\dagger b^j$. Integrating it with respect to time and taking the statistical average we end up with the following,

$$\begin{aligned} C^{kij}(\boldsymbol{r},t) &= \tfrac{1}{2}\{(g^{kl}(\boldsymbol{r},t) - g^{kl}(\boldsymbol{0},t))H^{ij}_{,l}(\boldsymbol{r},t) - g^{kj}_{,l}(\boldsymbol{r},t)H^{il}(\boldsymbol{r},t) - g^{ki}_{,l}(\boldsymbol{0},t)H^{lj}(\boldsymbol{r},t) \\ &+ \mathrm{i}k_z H^{ij}(\boldsymbol{r},t)(g^{k3}(\boldsymbol{0},t) - g^{k3}(\boldsymbol{r},t))\}. \end{aligned} \tag{A 4}$$

We mention here that the Furutsu–Novikov theorem follows the Stratanovich interpretation of the noise as compared to Ito. Substituting the last expression for the triple point averages into the (A 4) and after some long but trivial calculation we can find the equation for $H^{ij}(r)$.

Now given the equation for H^{ij} that can be obtained from both (A 2) and (A 4), we look at constructing the equations for scalar functions of H^{ij}. The procedure to express the tensor H^{ij} in terms of the possible scalar functions is mentioned in Oughton *et al.* (1997). It can then be shown that the correlation tensor H^{ij} has the general form written out in (2.9). We mention here that only the mirror symmetric part of the correlation function H^{ij} is important in the discussion. This is because the helical part of the magnetic field is not coupled to the governing equations of the non-helical part. One simple way to see this is to take the (A 2), now we use the form of C^{kij} from (A 4). If we look at an equation governing the proper scalar function in H^{ij}, it can be made up of two kinds of terms. One form of the term is a product of two proper scalar functions, more precisely a product of one proper scalar function in g^{ij} and one in H^{ij}. The other way is to construct it using the product of two pseudo scalar functions, one pseudo scalar function in g^{ij} and the other from H^{ij}. Since there are no pseudo scalar functions in g^{ij} the pseudo scalar functions in H^{ij} do not enter the governing equations of the proper scalar functions in H^{ij}. Hence we consider the magnetic correlation function H^{ij} made of only the proper scalar terms, H_{LL}, H_{NN}, H_Z, H_c. Due to the solenoidal condition we stick with two of these quantities H_{LL}, H_c and their governing equation derived using (A 2), (A 4) is mentioned in (2.15).

Appendix B. Asymptotic forms for correlation functions

The small and large r forms for the correlation functions $h_{LL}(r)$ and $h_c(r)$ can be obtained from their governing equations (2.15). For the case of finite Rm the small r expression reads as,

$$h_{LL}(r) = a_0 - \frac{(\gamma + 2\eta k_z^2 - 8D_1)a_0 - 4\eta k_z b_1}{16\eta} r^2 + O(r^4), \tag{B 1}$$

$$h_c(r) = b_1 r - \frac{(\gamma + 2\eta k_z^2)b_1 - 2k_z D_2 a_0}{16\eta} r^3 + O(r^5); \tag{B 2}$$

here a_0, b_1 are constants. For the large r behaviour we have,

$$h_{LL}(r) \sim \mathrm{e}^{-\sqrt{\gamma/2\eta + k_z^2}\, r}, \tag{B 3}$$

$$h_c(r) \sim \mathrm{e}^{-\sqrt{\gamma/2\eta + k_z^2}\, r}. \tag{B 4}$$

For the case $Rm \to \infty$, we have the rescaled $\tilde{r} = rk_d$ and $\tilde{k}_z = k_z/k_d$. The small $\tilde{r}$ behaviours of the functions $h_{LL}(\tilde{r})$, $h_c(\tilde{r})$ obtained from (5.2) are,

$$h_{LL}(\tilde{r}) = \tilde{a}_0 - \frac{(\gamma + 2\tilde{k}_z^2 - 8)\tilde{a}_0 - 4\tilde{k}_z \tilde{b}_1}{16} \tilde{r}^2 + O(\tilde{r}^4), \tag{B 5}$$

$$h_c(\tilde{r}) = \tilde{b}_1 \tilde{r} - \frac{(\gamma + 2\tilde{k}_z^2)\tilde{b}_1 - 2\tilde{k}_z D_r \tilde{a}_0}{16} \tilde{r}^3 + O(\tilde{r}^5), \tag{B 6}$$

where $\tilde{a}_0, \tilde{b}_1$ are constants. For large $\tilde{r}$ we have,

$$h_{LL}(\tilde{r}) \sim \mathrm{e}^{-\sqrt{D_r}\tilde{k}_z \tilde{r}}, \tag{B 7}$$

$$h_c(\tilde{r}) \sim \mathrm{e}^{-\sqrt{D_r}\tilde{k}_z \tilde{r}}. \tag{B 8}$$

Appendix C. Spectra of the eigenmode

From the asymptotics we can calculate the power laws of the isotropic spectra of the eigenmode. Using the asymptotic expression from the previous section we reconstruct the following form for the correlation functions $h_{LL}(r)$, $h_c(r)$:

$$h_{LL}(r) = \mathrm{e}^{-\sqrt{D_r}k_z r} \sum_{n=0}^{\infty} h_n r^{2n}, \tag{C 1}$$

$$h_c(r) = \mathrm{e}^{-\sqrt{D_r}k_z r} \sum_{n=0}^{\infty} g_n r^{2n}. \tag{C 2}$$

Now we look for the behaviour of $E^B_{2D}(k)$, $E^B_Z(k)$ for $k \ll k_z$ and $k \gg k_d$. The intermediate range of scales when there is sufficient scale separation between k_z and k_d will be dealt with using matched asymptotics. The details of the calculation and the resulting scaling in this intermediate range are mentioned in the following appendix section (see appendix D). Using the expression (C 2) we can obtain an expression for $E^B_{2D}(k)$, $E^B_Z(k)$ in the small $k \ll k_z$ limit,

$$E^B_{2D}(k) = c_1 \frac{k}{k_z} + O(k^3), \tag{C 3}$$

$$E^B_Z(k) = c_2 \frac{k^3}{k_z^3} + O(k^3), \tag{C 4}$$

where c_1 and c_2 are some constants that are independent of k. For scales larger than the dissipative scales $k \gg k_d$ we need to look at the small r behaviour for h_{2D}, h_Z. We use the steepest descent method for the correlation functions in (C 2) and obtain the following,

$$E^B_{2D}(k) = \mathrm{e}^{-k/k_d}(\tilde{c_1} + O(k^{-3/2})), \tag{C 5}$$

$$E^B_{Z}(k) = \mathrm{e}^{-k/k_d}(\tilde{c_2} + O(k^{-3/2})), \tag{C 6}$$

where $\tilde{c}_1$ and $\tilde{c}_2$ are some constants independent of k. These behaviour are well captured in the results from the eigenvalue solver (see figure 5).

Appendix D. Matched asymptotics

We are interested in finding the behaviour of the functions E^B_{2D}, E^B_Z in the intermediate region $k_z \ll k \ll k_d$. In this process we would like to find the value of γ in the limit of $k_z \ll k_d$. From the numerics we can see that the value of γ is 3 in the limit of small k_z and independent of the value of D_r, see figures 1 and 3. We are interested in the limit $Rm \to \infty$ the governing equations are given by (5.2). Since the equation is rescaled with k_d the small parameter now is $\tilde{k}_z \ll 1$. The idea here is to find the inner solution of the equation by expanding in terms of powers of $\tilde{k}_z$ the (5.2). Then we compute the outer solution by rescaling the variable $\tilde{r}$ to $\hat{r} = \sqrt{D_r} k_z \tilde{r}$. This rescaling would then provide us with a new set of equations for the outer solution. The behaviour of the inner solution is valid in the region $\tilde{r} \ll 1$ while the outer solution is valid in the region $\tilde{r} \gg 1/\tilde{k}_z$. The matching will take place in the intermediate range of scales, to get the exponents and the eigenvalue γ.

D.1. *Inner solution*

We do asymptotics for $\tilde{k}_z \ll 1$ with $h_{LL} = H_0 + \tilde{k}_z^2 H_1 + \cdots$ and $h_c = D_r \tilde{k}_z (G_0 + \tilde{k}_z^2 G_1 + \cdot)$, the equation for zeroth order in $\tilde{k}_z$ satisfies,

$$\tilde{r}^2 \left[H_0'' + 7\frac{H_0'}{\tilde{r}} - (\gamma - 8)\frac{H_0}{\tilde{r}^2} \right] + \left[2H_0'' + 6\frac{H_0'}{\tilde{r}} \right] = 0, \tag{D 1}$$

$$\tilde{r}^2 \left[G_0'' + \frac{G_0'}{\tilde{r}} - (\gamma + 1)\frac{G_0}{\tilde{r}^2} \right] + \left[2G_0'' + 2\frac{G_0'}{\tilde{r}} - 2\frac{G_0}{\tilde{r}^2} \right] = 2\tilde{r} H. \tag{D 2}$$

Now we write the homogeneous solution to the equations using hypergeometric functions ${}_2F_1$ defined as ${}_2F_1(a, b, c, d) = \Gamma(c)/(\Gamma(b)\Gamma(c-b)) \int_0^1 t^b (1-t)^{c-b-1}/(1-tz)^a \, \mathrm{d}t$,

$$H_0(\tilde{r}) = C_1 \, {}_2F_1 \left[\frac{3}{2} - \frac{\sqrt{1+\gamma}}{2}, \frac{3}{2} + \frac{\sqrt{1+\gamma}}{2}, 2; -\frac{\tilde{r}^2}{2} \right], \tag{D 3}$$

$$G_{0H}(\tilde{r}) = C_2 \, \tilde{r} \, {}_2F_1 \left[\frac{1}{2} - \frac{\sqrt{1+\gamma}}{2}, \frac{1}{2} + \frac{\sqrt{1+\gamma}}{2}, 2; -\frac{\tilde{r}^2}{2} \right], \tag{D 4}$$

where $G_0 = G_{0H} + G_{0I}$ with G_{0H} the homogeneous solution and G_{0I} the inhomogeneous solution. G_{0I} can be found and expressed in terms of integrals using the Wronskian. The asymptotics for large $\tilde{r}$ is found to be,

$$G_{0I}(\tilde{r}) = C_1 \frac{1}{(\gamma+1)} \tilde{r}^{-2\sqrt{\gamma+1}}. \tag{D 5}$$

D.2. *Outer solution*

For the large $\tilde{r}$ limit we could rescale $\hat{r} \to \tilde{k}_z \tilde{r}$ but in order to get rid of the dependence on D_r at the lowest order we do the following rescaling, $\hat{r} \to \sqrt{D_r}\tilde{k}_z \tilde{r}$. This ends up with the following set of equations,

$$\gamma h_{LL} - (2D_r\tilde{k}_z^2 + \hat{r}^2)[h_{LL}'' + 3\frac{h_{LL}}{\hat{r}}] + (2\tilde{k}_z^2 + \hat{r}^2)h_{LL} = 8h_{LL} + 4\hat{r}h_{LL}' + 8\frac{\hat{r}}{\sqrt{D_r}}h_c + \frac{4}{\hat{r}}\sqrt{D_r}\tilde{k}_z^2 h_c, \tag{D 6}$$

$$\gamma h_c - (2D_r\tilde{k}_z^2 + \hat{r}^2)\left[h_c'' + \frac{h_c'}{\hat{r}} - \frac{h_c}{\hat{r}^2}\right] + (2\tilde{k}_z^2 + \hat{r}^2)h_c = 2\hat{r}\sqrt{D_r}h_{LL}. \tag{D 7}$$

Since $\tilde{k}_z \ll 1$ we can again expand the quantities $H_{LL}(\hat{r})$, $H_c(\hat{r})$ in powers of $\tilde{k}_z$,

$$h_{LL} = [\hat{H}_0(\hat{r}, \gamma) + \tilde{k}_z^2\hat{H}_1(\hat{r}, \gamma, \tilde{k}_z, \sqrt{D_r}) + \tilde{k}_z^4\hat{H}_2(\hat{r}, \gamma, \sqrt{D_r}) + \cdots], \tag{D 8}$$

$$h_c = \sqrt{D_r}[\hat{G}_0(\hat{r}, \gamma) + \tilde{k}_z^2\hat{G}_1(\hat{r}, \gamma, \sqrt{D_r}) + \tilde{k}_z^4\hat{G}_2(\hat{r}, \gamma, \sqrt{D_r}) + \cdots]. \tag{D 9}$$

With this expansion the equation at the leading order becomes independent of D_r with the assumptions being $D_r\tilde{k}_z^2 \ll 1, \tilde{k}_z^2 \ll 1$. The leading-order equations are,

$$(\gamma - 8)\hat{H}_0 - \hat{r}^2\left[\hat{H}_0'' + 3\frac{\hat{H}_0'}{\hat{r}}\right] + \hat{r}^2\hat{H}_0 - 4\hat{r}\hat{H}_0' = 8\hat{r}\hat{G}_0, \tag{D 10}$$

$$\gamma\hat{G}_0 - \hat{r}^2\left[\hat{G}_0'' + \frac{\hat{G}_0'}{\hat{r}} - \frac{\hat{G}_0}{\hat{r}^2}\right] + \hat{r}^2\hat{G}_0 = 2\hat{r}\hat{H}_0. \tag{D 11}$$

The small $\hat{r}$ behaviour of the functions $\hat{H}_0$, $\hat{G}_0$ can be obtained by expanding in powers of $\hat{r}$. By direct substitution it can be shown that a simple power-law expansion fails for any value of γ and the expansion for small $\hat{r}$ contains logarithmic corrections.

D.3. *Matching*

We have to rescale the inner and outer variable to match the solutions at an intermediate range. The large r form for the inner solution reads like,

$$H_0(r) = r^{-\sqrt{1+\gamma}}\left[f_1(\gamma)\frac{1}{r^3} + f_2(\gamma)\frac{1}{r^5} + O\frac{1}{r^7}\right] + r^{\sqrt{1+\gamma}}\left[m_1(\gamma)\frac{1}{r^3} + m_2(\gamma)\frac{1}{r^5} + O\frac{1}{r^7}\right], \tag{D 12}$$

$$G_0(r) = r^{1-\sqrt{1+\gamma}}\left[\tilde{f}_1(\gamma)\frac{1}{r} + \tilde{f}_2(\gamma)\frac{1}{r^3} + O\frac{1}{r^5}\right] + r^{1+\sqrt{1+\gamma}}\left[\tilde{m}_1(\gamma)\frac{1}{r} + \tilde{m}_2(\gamma)\frac{1}{r^3} + O\frac{1}{r^5}\right] \tag{D 13}$$

for $\gamma \neq 3$. For $\gamma = 3$ the coefficients f_i, m_i and $\tilde{f}_i$, $\tilde{m}_i$ diverge. In this case the expansion involves logarithmic corrections to the power laws. A successful matching with the outer solution (that also includes logarithmic corrections) becomes only possible for $\gamma = 3$. The power-law behaviours for the correlation functions are then a direct consequence of this eigenvalue and the properties of the hypergeometric

functions. Thus in the intermediate region $r_d \ll r \ll 1/k_z$ the solution has the exponents $h_{LL} \sim r^{-1}$, $h_c \sim \sqrt{D_r}k_z r^0$. Using Wiener–Khintchine we can find the corresponding behaviour in the spectral space to be, $E^B_{2D} \sim k^0 + \sqrt{D_r}k_z/k^2/2$ and $E^B_Z(k) \sim \sqrt{D_r}k_z k^0/2$.

REFERENCES

BOLDYREV, S. 2001 A solvable model for nonlinear mean field dynamo. *Astrophys. J.* **562** (2), 1081.

BOLDYREV, S., CATTANEO, F. & ROSNER, R. 2005 Magnetic-field generation in helical turbulence. *Phys. Rev. Lett.* **95** (25), 255001.

BOLDYREV, S. A. & SCHEKOCHIHIN, A. A. 2000 Geometric properties of passive random advection. *Phys. Rev.* E **62** (1), 545.

CHATFIELD, C. 1989 *The Analysis of Time Series an Introduction*. Chapman and Hall.

CHERTKOV, M., FALKOVICH, G., KOLOKOLOV, I. & VERGASSOLA, M. 1999 Small-scale turbulent dynamo. *Phys. Rev. Lett.* **83** (20), 4065.

FALKOVICH, G., GAWDZKI, K. & VERGASSOLA, M. 2001 Particles and fields in fluid turbulence. *Rev. Mod. Phys.* **73** (4), 913.

FURUTSU, K. 1963 On the statistical theory of electromagnetic waves in a fluctuating medium (i). *J. Res. Natl Bur. Stand.* **67D**, 303.

GALLOWAY, D. J. & PROCTOR, M. R. E. 1992 Numerical calculations of fast dynamos in smooth velocity fields with realistic diffusion. *Nature* **356**, 691–693.

GREINER, A., STRITTMATTER, W. & HONERKAMP, J. 1988 Numerical integration of stochastic differential equations. *J. Stat. Phys.* **51** (1–2), 95–108.

ISKAKOV, A. B., SCHEKOCHIHIN, A. A., COWLEY, S. C., MCWILLIAMS, J. C. & PROCTOR, M. R. E. 2007 Numerical demonstration of fluctuation dynamo at low magnetic Prandtl numbers. *Phys. Rev. Lett.* **98** (20), 208501.

KAZANTSEV, A. P. 1968 Enhancement of a magnetic field by a conducting fluid. *Sov. Phys. JETP* **26** (5), 1031–1034.

KOLOKOLOV, I. 2016 Kinematic dynamo in two-dimensional chaotic flow: the initial and final stages. arXiv:1603:08771.

KRAICHNAN, R. H. 1968 Small-scale structure of a scalar field convected by turbulence. *Phys. Fluids* **11** (5), 945–953.

LEPROVOST, N. 2004, Influence des petites échelles sur la dynamique à grande échelle en turbulence hydro et magnétohydrodynamique. PhD thesis, Université Pierre et Marie Curie-Paris VI.

MALYSHKIN, L. M. & BOLDYREV, S. 2010 Magnetic dynamo action at low magnetic Prandtl numbers. *Phys. Rev. Lett.* **105** (21), 215002.

MASON, J., MALYSHKIN, L., BOLDYREV, S. & CATTANEO, F. 2011 Magnetic dynamo action in random flows with zero and finite correlation times. *Astrophys. J.* **730** (2), 86.

NOVIKOV, E. A. 1965 Functionals and the random-force method in turbulence theory. *Sov. Phys. JETP* **20** (5), 1290–1294.

NOVIKOV, V. G., RUZMAIKIN, A. A. & SOKOLOFF, D. D. 1983 Kinematic dynamo in a reflection-invariant random field. *Sov. Phys. JETP* **58**, 527–532.

OUGHTON, S., RÄDLER, K. H. & MATTHAEUS, W. H. 1997 General second-rank correlation tensors for homogeneous magnetohydrodynamic turbulence. *Phys. Rev.* E **56** (3), 2875.

PROUDMAN, J. 1916 On the motion of solids in a liquid possessing vorticity. *Proc. R. Soc. Lond.* A **92** (642), 408–424.

ROBERTS, G. O. 1972 Dynamo action of fluid motions with two-dimensional periodicity. *Phil. Trans. R. Soc.* **271** (1216), 411–454.

RUZMAIKIN, A. A. & SOKOLOV, D. D. 1981 The magnetic field in mirror-invariant turbulence. *Sov. Astron. Lett.* **7**, 388–390.

SCHEKOCHIHIN, A. A., BOLDYREV, S. A. & KULSRUD, R. M. 2002 Spectra and growth rates of fluctuating magnetic fields in the kinematic dynamo theory with large magnetic Prandtl numbers. *Astrophys. J.* **567** (2), 828.

SCHEKOCHIHIN, A. A., COWLEY, S. C., TAYLOR, S. F., MARON, J. L. & MCWILLIAMS, J. C. 2004 Simulations of the small-scale turbulent dynamo. *Astrophys. J.* **612** (1), 276.

SESHASAYANAN, K. & ALEXAKIS, A. 2016 Turbulent 2.5-dimensional dynamos. *J. Fluid Mech.* **799**, 246–264.

SMITH, S. G. L. & TOBIAS, S. M. 2004 Vortex dynamos. *J. Fluid Mech.* **498**, 1–21.

SUBRAMANIAN, K. 1999 Unified treatment of small-and large-scale dynamos in helical turbulence. *Phys. Rev. Lett.* **83** (15), 2957.

TAYLOR, GO. I. 1917 Motion of solids in fluids when the flow is not irrotational. *Proc. R. Soc. Lond.* A **93** (648), 99–113.

TOBIAS, S. M. & CATTANEO, F. 2008 Dynamo action in complex flows: the quick and the fast. *J. Fluid Mech.* **601**, 101–122.

VINCENZI, D. 2002 The Kraichnan–Kazantsev dynamo. *J. Stat. Phys.* **106** (5–6), 1073–1091.

ZELDOVICH, Y. B. 1957 The magnetic field in the two-dimensional motion of a conducting turbulent fluid. *Sov. Phys. JETP* **4**, 460–462.